Generation of Standard EM Fields Using TEM Transmission Cells

MYRON L. CRAWFORD

Abstract—**A new technique developed at the National Bureau of Standards (NBS) for establishing standard, uniform, electromagnetic (EM) fields in a shielded environment is described. The technique employs transverse electromagnetic (TEM) transmission cells that operate as 50 Ω impedance-matched systems. A uniform TEM field is established inside a cell at any frequency of interest below that for which higher order modes begin to propagate. Standard field strength levels from 10 μV/m to 500 V/m can be established with uncertainties of less than 1.0 dB to 2.0 dB inside the NBS cells for frequencies from dc to 500 MHz. The cells are especially useful for calibrating EM radiation hazard meters, for emission and susceptibility testing of small to medium sized equipment, and for special low level calibration of very sensitive field strength meters.**

I. INTRODUCTION

THE proliferation of electronic/electromechanical systems in our environment is causing a rapid rise in the level and number of potential interfering signals. Compatible operation of such systems in the presence of electromagnetic (EM) interference is a function of their EM susceptibility, the ability to accurately measure and control it, and/or to effectively shield against it.

A number of techniques exist for establishing known, uniform levels of electromagnetic energy for susceptibility testing over limited frequency ranges and for limited applications [1]–[3]. For example, high level fields can be generated quite accurately above a few hundred megahertz using standard gain horns and below a few megahertz using parallel plate lines. Both these techniques are widely used, but suffer a major disadvantage; they radiate electromagnetic energy into the surrounding space which may interfere with the measurements, be hazardous to the operator, or interfere with other experiments being conducted within transmission range.

The technique described in this paper contains the EM field inside the transmission cell. It is extremely broad band in frequency, being limited only by the waveguide multimode frequency associated with the cell size. Construction costs of the cells are minimal and the use of expensive anechoic chambers or shielded enclosures are unnecessary. The cells can be used to establish known field strength levels from 10 μV/m to 500 V/m with uncertainties less than 1.0 dB to 2.0 dB (depending on frequency). The cells are especially useful for calibrating EM radiation hazard monitors, for equipment emissions and susceptibility testing, and for special low-level sensor calibrations.

Manuscript received April 16, 1974.
The author is with the National Bureau of Standards, Boulder, Colo. 80302.

II. DESCRIPTION, DESIGN, AND EVALUATION OF THE TEM CELLS

The design of the cells was patterned somewhat after a large cell constructed for the USAF School of Aerospace Medicine at Brooks AFB [4]. The NBS cells were designed as shielded chambers for EM susceptibility and emissions testing of test specimens, and for calibration of EM field probes. A cross sectional view of a typical cell is shown in Fig. 1. The cell consists of a section of rectangular coaxial transmission line tapered at each end to adapt to standard coaxial connectors. The line and tapered transitions have a nominal characteristic impedance of 50 ohms along their length to insure minimum voltage standing wave ratios (VSWR). The EM field is developed inside the cell when RF energy is coupled to the line from a transmitter connected at the cell input port. A matched 50 ohm termination is connected to the output port. The fields inside the cell are monitored using special electric and magnetic field probes designed and constructed by NBS [5]. A differential power measuring system, designed by NBS [6] for measuring energy absorbed from the cell by test subjects, can also be used to determine the field strength if the cell's impedance is known.

Experience with the Brooks AFB cell showed that at frequencies for which only the principal wave (TEM mode) propagates through the cell, a reasonably uniform electric field could be generated. The main limitation of their cell was its large size, restricting its usefulness to frequencies below 50 MHz. A series of smaller cells were developed at NBS to increase this range up to 500 MHz. The major design considerations were:

1) maximize usable test cross sectional area;
2) maximize upper useful frequency limit;
3) minimize cell impedance mismatch or voltage standing wave; and
4) maximize uniformity of EM field pattern characteristic of the cell.

The cells were designed using experimental modeling and the approximate equation for the characteristic impedance of shielded strip line [4]

$$z_0 \simeq \frac{94.15}{(\epsilon_r)^{1/2}\left[\dfrac{w}{b(1-t/b)} + \dfrac{C_f'}{0.0885\epsilon_r}\right]} \quad \text{(ohms)} \quad (1)$$

where ϵ_r is the relative dielectric constant of the medium between the conductors, C_f' is the fringing capacitance in

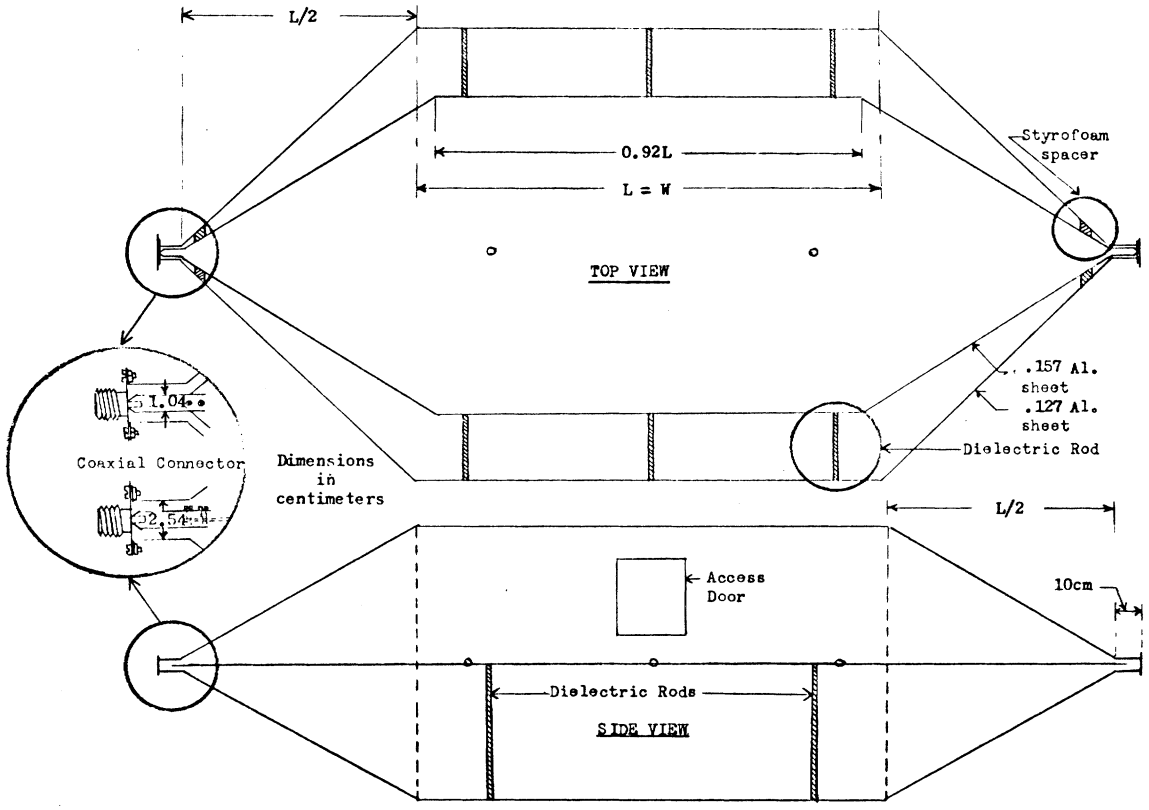

Fig. 1. Design for rectangular TEM transmission cell.

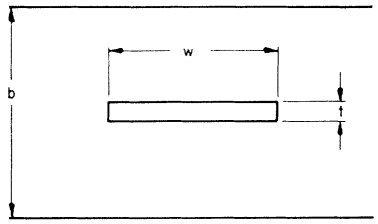

Fig. 2. Shielded strip line.

picofarads per centimeter, and w, b, and t are shown in Fig. 2.

The problem of modifying the shielded strip line into a "rectangular coaxial" line was primarily one of determining experimentally the value of C_f'. This was done using a time domain reflectometer (TDR) to evaluate small scale models of cells with the cross sectional geometry shown in Figs. 3 and 4. C_f' was found to be approximately equal to 0.087 pF/cm, respectively. Dimensions for b were determined from the design criterion that as much as 1/3 [1] of the volume between the septum and outer plates can be occupied by the equipment under test (EUT) to meet design considerations 1, 3, and 4. Once b was calculated, an experimental estimate of C_f' determined, and an available metal thickness t selected, w can be calculated from (1), assuming a nominal 52 ohms for the line characteristic impedance. (Fifty-two ohms

[1] The one third factor is considered a maximum. The impedance loading effect from inserting the EUT should not exceed a few ohms if a reasonable VSWR and EM field perturbation is to be maintained.

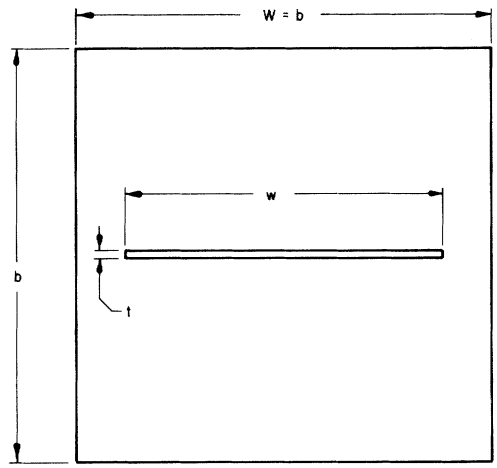

Fig. 3. Cross sectional view of optimum geometry of rectangular transmission line for maximum test area and frequency.

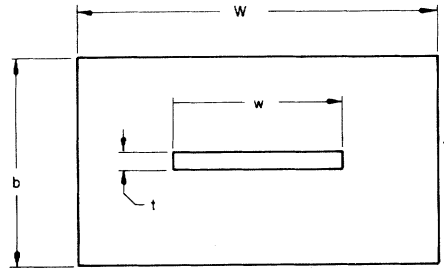

Fig. 4. Cross sectional view of rectangular transmisison line with improved E field uniformity.

TABLE 1
TEM CELL DIMENSIONS

Cutoff/ Multimode Frequency (MHz)	Square Cell (Fig. 3) Plate Separation b (cm)	w (cm)	t (cm)	C'_f (pF/cm)	Rectangular Cell (Fig. 4) Plate Separation b (cm)	w (cm)	t (cm)	C'_f (pF/cm)
100	150	123.83	.157	.087	90	108.15	.157	.053
300	50	41.28	.157	.087	30	36.05	.157	.053
500	30	24.77	.157	.087	18	21.83	.157	.053

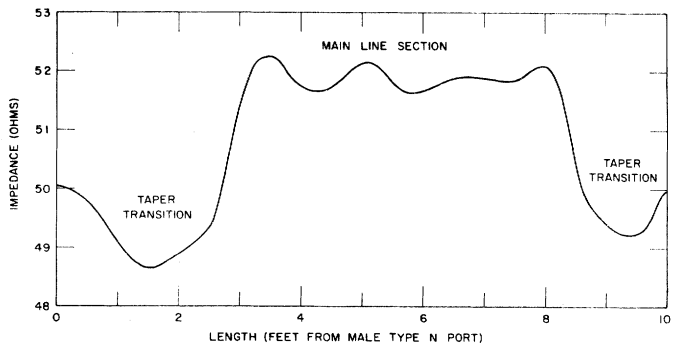

Fig. 5. Time domain reflectometer trace of distributed impedance of empty cell. (Form factor Fig. 3.)

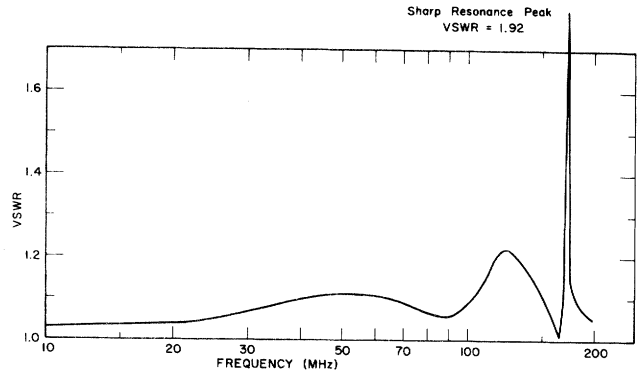

Fig. 6. Port input VSWR of empty cell. (Form factor Fig. 3.)

was chosen to allow for some impedance loading effect when inserting the EUT inside the cell.) Table 1 gives the dimensions for constructing the two cell forms with specified upper frequency limits. The TDR was then used to make refinements by trimming w until the proper characteristic impedance was obtained.

The cross section of Fig. 3 is used at high frequencies where maximum cell size is limited and requires some compromise in electric field uniformity. The cross section of Fig. 4 achieves greater field uniformity at the cost of vertical test space restriction. Fig. 5 gives a typical TDR trace of the distributed impedance along the length of a cell of Fig. 3 cross section, and Fig. 6 shows the VSWR as seen at the cell's input and output ports.

MAPPING THE FIELDS INSIDE THE CELLS

Measurements were made using a calibrated short dipole to probe the electric field inside the empty cells. The variations in relative field strength versus position were determined in the longitudinal, transverse, and vertical directions within the cells. The electric field E is essentially vertically polarized in the region near the center of the cells and gradually becomes horizontally polarized as one moves in the horizontal direction toward the gap at the side. Both vertical and horizontal components of E were measured at each point to determine the total electric field, $E = (E_v^2 + E_H^2)^{1/2}$ where E_v and E_H are in phase. The electric field distributions for each form factor are shown in Figs. 7 and 8. The electric field in the test regions shown is primarily vertically polarized or $E_v \gg E_H$. The relative field distribution is independent of the magnitude of the test field used and the frequency so long as the frequency is less than the first order TE mode (TE_{10}) cutoff frequency given by the following equation:

$$(f_c)_{10} = c/2W. \tag{2}$$

The equation for determining the cutoff frequency for any higher order mode in general is given by

$$(f_c)_{m,n} = \frac{c(b^2m^2 + W^2n^2)^{1/2}}{2bW}. \tag{3}$$

For (2) and (3), c is the velocity of propagation of light $\simeq 3.0 \times 10^8$ m/s, b and W are as shown on Figs. 5 and 6, and m and n are integers related to the half sine variations of the field in the vertical and transverse directions. If higher order modes are allowed to propagate, the field configuration, which is the vector sum of each contributing mode, no longer has the simple pattern shown in Figs. 7 and 8. Thus higher order modes would greatly complicate interpretation of the measured results of the cell.

Variations in the electric field strength for the empty cells were less than 2 dB for the cross section of Fig. 3 and less than 1 dB for the cross section of Fig. 4 over the area typically occupied by the EUT. Inserting the EUT shorts out part of the electric field due to the metal in the case and increases the field strength proportional to the percentage cross section occupied. Fig. 9 shows an example of the results of inserting a solid metal case inside a cell of the form factor shown in Fig. 3. This case occupied 1/3 the vertical separation between the upper wall and

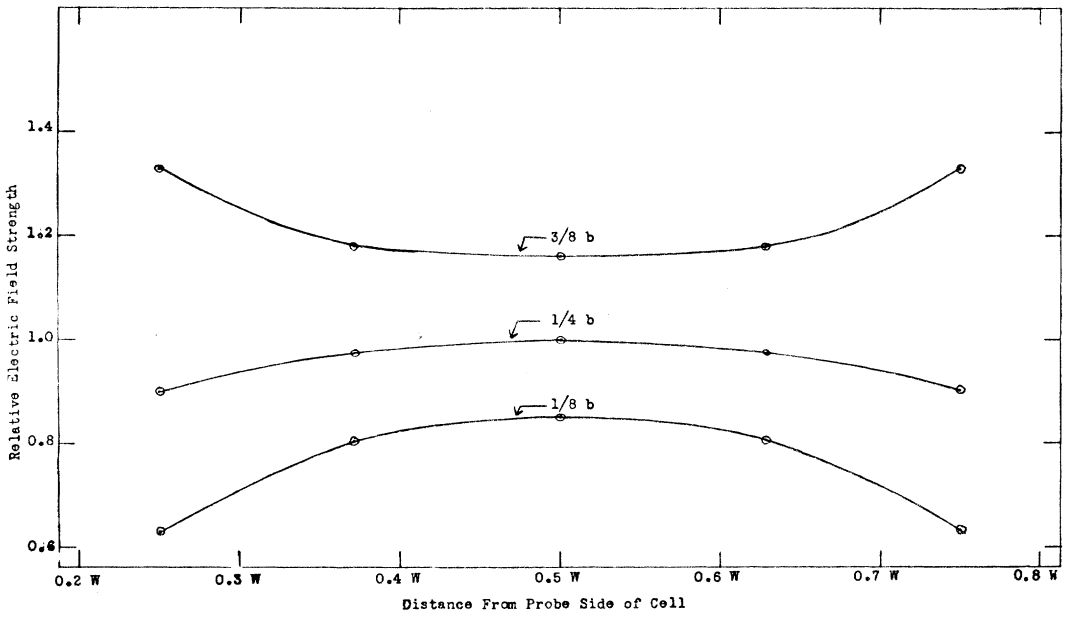

Fig 7. Relative electric field distribution inside cell. Cross sectional cut through upper half at center of cell. (Form factor Fig. 3.)

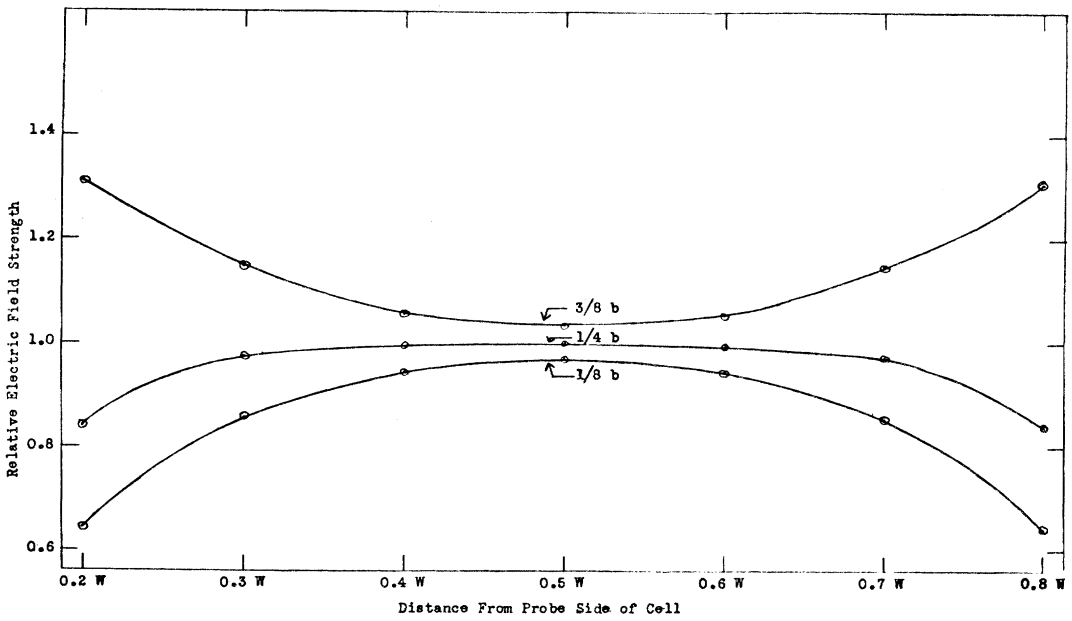

Fig. 8. Relative electric field distribution inside cell. Cross sectional cut through upper half at center of cell. (Form factor Fig. 4.)

the septum or center conductor and increased the field strength 3 dB and 6 dB, respectively, in the regions directly above and below the case. This increase in field strength for a constant test input power must be taken into account when determining the absolute test field, and occurs if significant cross section within the cell is occupied by the EUT.

III. STANDARDIZATION OF THE FIELD INSIDE THE CELLS

The absolute electric field strength E_v at the cell's center between the upper wall and the center conductor is determined using the equation

$$E_v = (P_n R_c)^{1/2}/d \tag{4}$$

where P_n is the net power flowing through the cell, R_c is the real part of the cell's complex characteristic impedance, and d is the separation distance between the cell's upper wall and its center plate or septum.

A brief discussion of the sources of error is given below. The total fractional error ΔE_v in determining the absolute field strength E_v inside the cell is given as

$$\Delta E_v \simeq | \tfrac{1}{2}(\epsilon_R + \epsilon_P) + \epsilon_d + \epsilon_E | \tag{5}$$

where $\epsilon_P = \Delta P_n/P_n$, $\epsilon_R = \Delta R_c/R_c$, $\epsilon_d = \Delta_d/d$, and ϵ_E is the error due to the nonuniformity of E_v determined experimentally by mapping the field distribution in the test region of the cell. Equation (5) was derived by substituting $P_n' = | P_n + \Delta P_n |$, $R_c' = | R_c + \Delta R_c |$, and

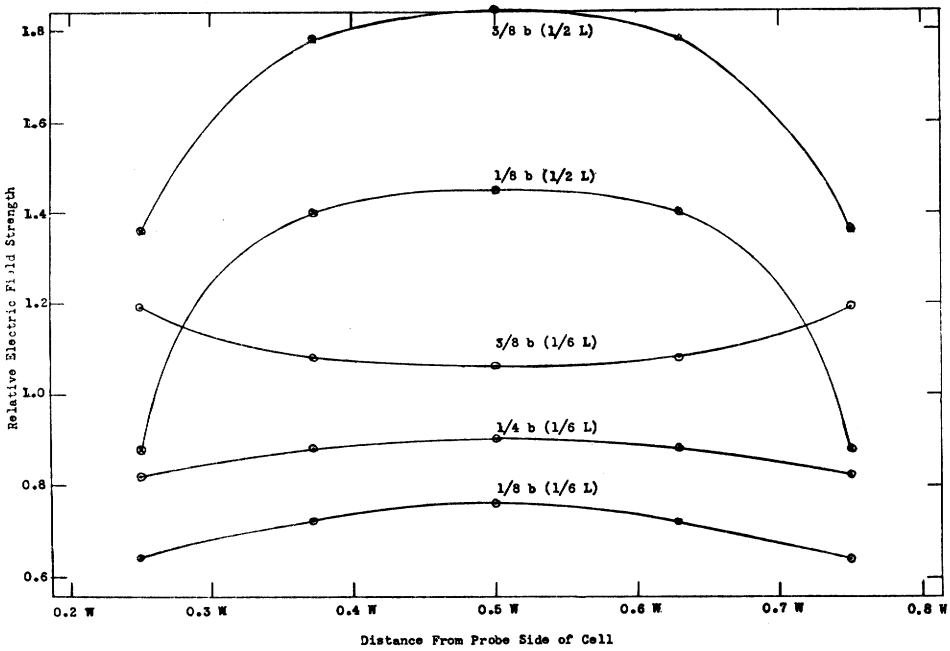

Fig. 9. Relative electric field distribution inside cell with metal case mounted in center of upper half space. Cross sectional cuts at center and off end of case.

$d' = | d + \Delta d |$ into (4) and adding ϵ_E (obtained from E field mapping). Higher order terms contributing to small errors were then dropped in the derivation to arrive at (5).

The error ϵ_P, in determining P_n, is due to uncertainties in coupler calibration, absolute measurement of RF power on the side arm of the coupler, and impedance mismatch between the cell, coupler, RF source, and cell termination. If a precision calibrated coupler and power meter are used and the cell and its termination are impedance matched (VSWR $\leq$ 1.05), ϵ_P should be less than $\pm 5\%$.

The error ϵ_R in determining R_c is a function of the measurement accuracy of the TDR and the impedance loading of the EUT inside the cell. If the EUT occupies a small portion ($\leq 1/5$) of the cross section of the cell, ϵ_R will be small ($\leq 3\%$), and is typically neglected in the calculation of E_v. For larger EUT's (occupying up to 1/3 the cross section of the cell) the impedance loading effect must be determined with the TDR and used to correct R_c when using (4) to calculate E_v. ϵ_R for these cases can be much larger but typically would be less than 10% if the EUT is centered inside the cell. Exceeding the 1/3 load factor is not recommended.

Determining ϵ_E is more difficult. Introducing the EUT inside the cell perturbs the electric field distribution as described in the section on field mapping. This loading factor (increase in E) is determined using the small calibrated probes referred to earlier. If the size of the EUT is less than the 1/5th factor and if care is taken to properly orient or eliminate interconnecting leads to the EUT, ϵ_E can be reduced to less than 6% for cells with the form factor of Fig. 3. Larger EUT's would necessitate measurement of the field distribution around the EUT and a resulting higher estimate of ϵ_E.

TABLE 2
SUMMARY OF MEASUREMENT ERRORS

Source of Error	Percent Uncertainty: Form Factor Fig. 4	Form Factor Fig. 3
a) Absolute measurement of incident RF power on the side arm of coupler	± 3.0	± 3.0
b) Coupler calibration	± 2.0	± 2.0
ϵ_p, total error in determination of RF power passing through cell	± 5.0	± 5.0
c) Real part of cell complex impedance ϵ_R	± 3.0	± 3.0
d) Cell plate separation ϵ_d	± 1.0	± 1.0
e) Nonuniformity of electric field inside cell ϵ_E	± 6.0	±20.0
maximum field strength error	±11.0 <± 1.0 dB	±25.0 <± 2.0 dB

$$\Delta E_v \sim | \tfrac{1}{2}(0.03 + 0.05) + 0.01 + 0.06 | \times 100 \quad (0.20)$$

The sources of errors for the two form factors are summarized in Table 2.

IV. APPLICATIONS

The block diagrams for making EM susceptibility measurements using the cell are shown in Fig. 10. The EUT is mounted inside the cell in the desired orientation with the interconnecting leads/cables and power cord extended through a side or end wall of the cell, as required. The orientation, size, and type (shielded or unshielded) of interconnecting leads and power cord of the EUT can have a large effect upon the equipment's susceptibility. Tests can be performed with the leads oriented for minimum or maximum field coupling while making the

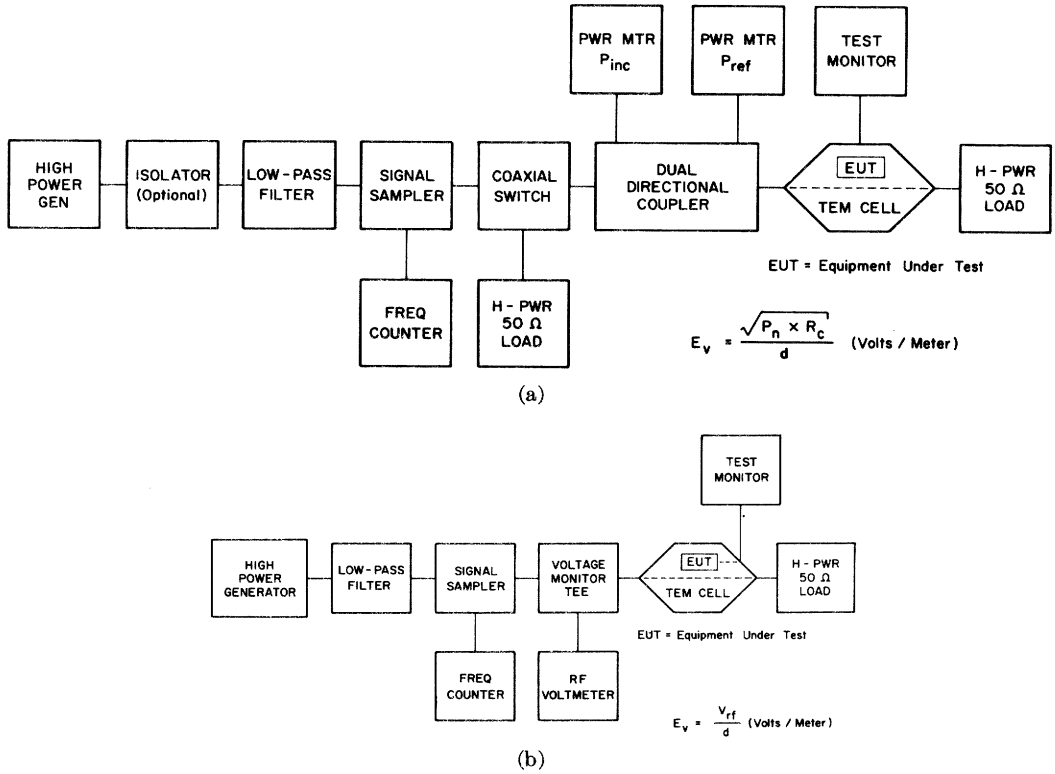

Fig. 10. Block diagrams of system for susceptibility testing of equipment.

susceptibility measurements, thus providing data for evaluating the lead contributions to the overall EUT susceptibility. Minimum lead interaction with the test field is achieved by orienting them in a direction perpendicular to the E field and by properly shielding them. Maximum interaction is achieved by allowing the unshielded leads to sag inside the cell and/or by aligning with the polarization of the test field (leads through top of cell). The susceptibility level for the EUT is determined at frequencies from 1 MHz to the cell multimode frequency by means of the block diagram of Fig. 10(a). The generator output is progressively increased until the EUT's normal operation is noticeably affected. The test field can be further increased until the EUT fails if failure tests are required.

The cells can also be used to calibrate various field detection devices such as hazard probes, field sensors, or small field intensity meters. In this type of operation the device being calibrated is placed inside the cell in a uniform field region. The standard test field is determined by the procedure outlined in Section III, and the field intensity indicated by the instrument is compared with the known value of the standard test field.

Measurements below 1 MHz are made using a voltage monitor tee and RF voltmeter as shown in Fig. 10(b), because directional couplers are not available at these lower frequencies. Directional couplers and power meters are used above 1 MHz because of the ability to monitor impedance variations in the system when installing EUT's inside the cell and orienting them for various tests.

Swept measurements can be made for a fixed orientation of the EUT and its cables using the block diagrams of Fig. 10(a) or (b) assuming the circuit components remain matched over the desired frequency range and have acceptable frequency bandwidth characteristics. When using the system of Fig. 10(b), the input voltage to the cell is monitored directly and (4) becomes,

$$E_v = V_c/d \tag{6}$$

where V_c is the measured input voltage to the cell and is equivalent to $V_c = (P_n R_c)^{1/2}$. The error analysis then involves evaluating the uncertainty in measuring V_c as compared to P_n and R_c, and at the frequencies indicated for these tests, the errors would be about equivalent.

Pulsed RF susceptibility measurements can also be made by replacing the signal source and monitor/detector with an appropriate pulse generator, sampler, and detector (oscilloscope). The exposure level standardization would be similar to that outlined in Section III, but would involve determining the calibration measurement accuracy of the detector, the sampling (coupling) accuracy, and the time domain response of the cell. Additional work needs to be done in this area but it is believed that measurements using pulses with frequency components less than 500 MHz could be made.

The measurement systems shown in Fig. 10(a) and (b) have been used to calibrate or determine the EM sus-

ceptibility of a number of test items. Examples are calibration and evaluation of radiation hazard probes and meters (both NBS and commercial types); calibration of small E field sensors; calibration of small field strength meters and sensitive receivers; susceptibility of fire alarms (smoke detectors) for malfunction and false alarm indication; equipment cable susceptibility (shielded and unshielded); and evaluation of RF conductance/interference on high resistance dc transmission lines.

Intercomparison of the standardized field strength data obtained using the cells with data taken using calibrated probes (calibrated with parallel plate lines and in a uniform field over a large ground screen) indicate excellent agreement, i.e., well within the uncertainties attributed to the different techniques. Table 3 presents a sample of these results at 15 MHz.

TABLE 3
INTERCOMPARISON ON NBS CELLS WITH PARALLEL PLATE LINE AT 16 MHz USING 10 cm DIPOLE PROBE

Probe Output Voltage	NBS 0.6 m by 1.0 m Cell E_v(V/m)	NBS 1.2 m by 1.2 m Cell E_v(V/m)	Parallel Plate Line E_v(V/m)
0.1	21.3	21.5	27.0
0.3	34.5	34.8	32.0
0.3	47.2	47.6	47.0
0.5	71.0	71.5	71.5
1.0	127.0	127.5	131

V. SUMMARY AND CONCLUSIONS

The objective of the work described in this paper was to develop an alternate technique for making susceptibility measurements of electronic equipment at frequencies up to 500 MHz. Tasks included designing and constructing the cells, optimizing the field distribution and usable test area inside the cells, evaluating the characteristics of the cell and measurement system, and performing susceptibility measurements on typical electronic equipment. The technique offers a unique way of determining not only EUT susceptibility to CW RF fields but also EUT susceptibility to pulsed RF fields. The cells can also be used to determine relative (as a function of frequency) levels of radiated emissions from electronic equipment by using the cell's inverse coupling characteristic with 50 ohm impedance-matched RF detectors connected to the input and/or output ports [7]. However, more work is needed to determine if these radiation measurements can be interpreted quantitatively.

The real advantage of using TEM transmission cells for making susceptibility or emissions measurements is the elimination of background interference without the introduction of measurement problems associated with shielded or anechoic enclosures. Furthermore, no EM fields are generated external to the cell and the cells produce uniform and readily determined fields. Shielded enclosures on the other hand reflect the emitted energy from their walls in such a complicated manner that prediction of the enhancement or interference of the desired signal is extremely difficult. Measurements using the cell are simple to make and require a minimum of detection equipment, e.g., no additional antennas are required.

The main handicap of the cell is its size limitation due to multimoding at higher frequencies. The largest cell at NBS can accomodate equipment 8 in by 19 in by 25 in at frequencies up to about 150 MHz. Smaller cells useful at frequencies up to 500 MHz have much less usable test space. Fig. 11 shows a photograph of the large NBS cell.

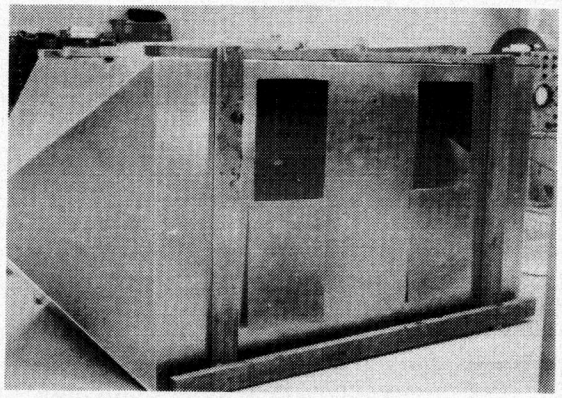

Fig. 11. Photograph of NBS rectangular TEM transmission cell.

VI. RECOMMENDATIONS FOR FUTURE WORK

Additional work is needed to solve the problems of size limitation of the cells, to evaluate the loading effects of large equipment inside the cells, to determine possible mode suppression and alteration techniques, and to derive the mathematics of cell modal coupling. The error analysis included in this report is rough and needs further refinement.

Only limited susceptibility measurements have been made using the cells. Additional measurements should be made with other pieces of equipment to establish the degree of generality of the method.

REFERENCES

[1] V. P. Musil, "Generating High-Intensity Electromagnetic Fields for Radiated-Susceptibility Test," *IEEE EMC Symp. Rec.*, Seattle, Wash., pp. 185–194, July 1968.
[2] B. E. Roseberry and R. B. Schulz, "A Parallel-Strip Line For Testing RF Susceptibility," *IEEE Trans. Electromagn. Compat.*, vol. EMC-7, pp. 142–150, June 1965.
[3] R. R. Bowman and W. E. Jessen, "Calibration Techniques for RAMCOR Densiometer Antennas," NBS Rep., unpublished, Dec. 1970.
[4] G. A. Skaggs, "High Frequency Exposure Chamber for Radiobiological Research, "NLR Memo. Rep. 2218, Feb. 1971.
[5] F. M. Greene, "Design and Calibration of E and H Field Probes for HF Band Application," *Proc. Dep. Defense Electromagnetic Res. Workshop*, Washington, D.C., pp. 50–76, Jan. 1971.
[6] M. L. Crawford, C. A. Hoer, and E. L. Komarek, "RF Differential Power Measurement System for the Brooks AFB Electromagnetic Radiation Hazards Experiment," NBS Rep. unpublished, Apr. 1971.
[7] M. L. Crawford, "Measurement of Electromagnetic Radiation from Electronic Equipment using TEM Transmission Cells," NBSIR 73-306, Feb. 1973.